COMPUTING THE MINIMAL REBINDING EFFECT INCLUDED IN A GIVEN KINETICS

M. WEBER AND K. FACKELDEY*

Abstract. In this article we show, that the binding kinetics of a molecular system can be identified by a projection of a continuous process onto a finite number of macro states. We thus interpret binding kinetics as a projection. When projecting onto non-overlapping macro states the Markovianity is spoiled. As a consequence, the description of e.g. a receptor-ligand system by a two state kinetics is not accurate. By assigning a degree of membership to each state, we abandon the non-overlapping approach. This overlap is crucial for a correct mapping of binding effects by Markov State Models with regard to their long time behavior. It enables us to describe the highly discussed rebinding effect, where the spatial arrangement of the system has the be included. By introducing a "degree of fuzziness" we have an indicator for the strength of the rebinding effect, such that the minimal rebinding effect can be derived from an optimization problem. The fuzziness also includes some new paradigms for molecular kinetics. These new model paradigms show good agreement with experimental data.

Key words. Conformation Dynamics, Molecular Kinetics, Rebinding, Recrossing, Cooperativity

AMS subject classifications. 15A15, 15A09, 15A23

1. Introduction.

Various authors from natural sciences have described and analyzed an effect which is denoted as rebinding effect (e.g. [Vau10, VL12, GAS+13, WBH12]). This topic has been discussed in the context of clustered receptors and clustered ligands in chemistry [CS11, MKMT05]. Whereas, in mathematical literature it is denoted as recrossing effect which has been investigated with respect to the spoiling of the Markov property in Markov State Models [EVE10, VET05, GR13]. In order to illustrate the meaning of this effect, think of a simple ligand-receptor binding process. In the simple case, this process can be characterized by a reaction equation

$$L + R \leftrightharpoons LR,$$

where the ligand (L) binds to a receptor (R) and forms a complex (LR). The ligand can be found in two different (macro)states – "bound" (LR) and "unbound" (L). According to this reaction one can derive kinetic constants, usually connected to an ordinary differential equation of the form

$$\dot{x}^T = x^T Q_c,$$

where $x^T = \frac{1}{s}(([L],[LR]))$, with $s = [L]+[LR] = \text{const.}$, is the time-dependent vector of the probabilities of the ligand to be bound or, respectively, to be unbound. These probabilities are proportional to the concentrations $[L]$ and $[LR]$. The matrix entries of Q_c are the rates of the reactions,

$$Q_c = \begin{pmatrix} -k_a[R] & k_a[R] \\ k_d & -k_d \end{pmatrix},$$

where k_a denotes the association and k_d the dissociation constant. This mathematical model of a binding kinetics comprises the Markov property. Given initial concentrations of the system, one can predict the future evolution of the concentration curves by

*Zuse Institute Berlin (ZIB), Takustr. 7, 14195 Berlin, Germany. {fackeldey, weber} zib.de

solving the ordinary differential equation (without knowing the "past"). The process seems to be without memory on the level of the two macro states.

This Makovian view on the macro scale is no longer justified when switching to the atomistic scale of a binding process. Here, the actual state depends still on the past, since a ligand having dissociated rebinds with a higher probability than a ligand being far away from the receptor. In other words, the spatial situation of the molecules is no longer negligible on the molecular scale and, thus, the accuracy of the discrimination between bound and unbound states is no longer sufficient.

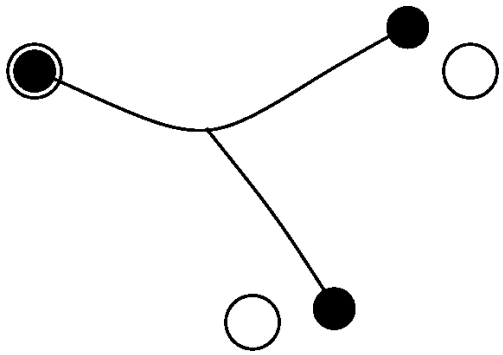

FIG. 1.1. *Sketch of a trivalent binding process being in a certain micro state: One part of the tivalent ligand is located in its binding site of a trivalent receptor, whereas the two other ligands are only "very near" to their binding sites. A strict classification of this micro state maybe impossible.*

Rao et al. [RLWW00] have synthesized a trivalent molecular system with a high binding affinity. Instead of giving thermodynamical reasons (lower entropy loss of a pre-organized ligand system), they claimed that the source of the high affinity is given by rebinding effects (Fig. 1.1). This means that the spatial arrangement of receptors and ligands leads to faster association and slower dissociation kinetics if the ligands approach the receptors. It is more likely that a ligand which unbinds will bind again before the whole ligand complex is dissociated from the receptor. This is a kind of memory effect included in the bound state of the system. This effect has also been discussed in the context of "configurational cooperativity" [Whi08]. We, therefore, suggest a model which enables to describe besides the bound and non-bound states also "intermediate" states, i.e. states between the bound and non-bound one [WBH12]. This is accomplished by assigning each micro state of the system a certain degree of membership to the both macro states (bound/non-bound), instead of just using a set based approach (see also [FRSW11] for a discussion). In this context we can, therefore, refer to a micro state as "almost bound" or "almost unbound".

This paper is structured as follows: In section two we show, how a molecular system can be explained in terms of transition rates between subsets of the conformational space. In section three we derive the minimal rebinding effect from a given kinetics by solving an optimization problem. In section four we show the performance of the method for some examples.

2. Molecular kinetics as a projection. In this article, we distinguish between micro states and macro states of a molecular system. A micro state of a molecular system with N atoms is represented in a $6N$ dimensional phase space, where $q \in \Omega = \mathbb{R}^{3N}$ are the spatial coordinates and $p \in \mathbb{R}^{3N}$ are the momenta. We assume that the

molecular system has an equilibrium distribution of micro states. One possible model is given by the Boltzmann distribution

$$\tilde{\rho}(q,p) \propto \exp(-\beta H(q,p)). \tag{2.1}$$

Here $\beta = 1/(k_B T)$ is the inverse temperature T multiplied with the Boltzmann constant k_B, and H denotes the Hamiltonian function which (in the classical, separable case) is given by $H(q,p) = K(p) + V(q)$, where $K(p)$ is the kinetic energy and $V(q)$ is the potential energy. By taking advantage of the fact, that the Boltzmann distribution π, can be decomposed as $\pi = \pi_p \pi_q$, where $\pi_p : \mathbb{R}^{3N} \to \mathbb{R}$ is the probability function of the kinetic part in the momentum space and $\pi_q : \Omega \to \mathbb{R}$ is the probability function of the potential part in the spatial coordinates Ω and by a suitable averaging of the momentum information we project the dynamics onto Ω. The corresponding reduced density $\pi_q = \int_{\mathbb{R}^N} \pi(q,p)\, dp$ is positive, finite and smooth. An ensemble of micro states is characterized by a density function $\tilde{\rho}(q,p)$, such that $\tilde{\rho}(q,p) dq \wedge dp$ gives the fraction of micro states in the volume element $dq \wedge dp$. This point of view motivates to group/cluster a "collection" of the micro states having the same or similar values in one observable [Sch99, DHFS00, DDJS99, DW05]. We call such a collection of micro states a macro state (e.g. "bound" or "unbound" state of a ligand-receptor-system). By grouping micro states, the macro states yield statistical weights and entropic information (regarding the corresponding part of the equilibrium density function). Macro states need not be distinct sets, we follow the approach of [Web06, DW05] by defining macro states as overlapping partial densities, which can be identified by membership functions $\chi_1, ..., \chi_n : \Omega \to [0,1]$, giving each vector of spatial coordinates q of a micro state a degree of membership to each macro state. These membership functions form a partition of unity, i.e.

$$\sum_{i=1}^{n} \chi_i(q) = 1.$$

This partition of Ω also allows us, to assign the statistical weights to each macro state, by

$$w_i = \int_\Omega \chi_i(q) \pi_q(q)\, dq. \tag{2.2}$$

The evolution of a time dependent density function $\rho : \mathbb{R} \times \Gamma \to \mathbb{R}$ of micro states $(q,p) \in \Gamma = \Omega \times \mathbb{R}^{3N}$ can then be given by an operator $\mathcal{F} : L^1(\Gamma) \to L^1(\Gamma)$:

$$\rho(t+\tau, \cdot) = \mathcal{F}_{t,\tau} \rho(t, \cdot), \tag{2.3}$$

where $t > 0$ is the time and τ is a time span. In the followings, we will consider the operator $\mathcal{F}$ in the case of an equilibrated molecular system. In this case, the time-dependence $\mathcal{F}_{t,\tau} = \mathcal{F}_\tau$ vanishes. The evolution (2.3) in the phase space can be projected onto the configuration space giving

$$\rho_q(t+\tau, \cdot) = \bar{\mathcal{P}}(\tau)\, \rho_q(t, \cdot), \tag{2.4}$$

where $\bar{\mathcal{P}}$ is a density propagating Markov operator and $\rho_q : \mathbb{R} \times \Omega \to \mathbb{R}$ is the time dependent projected density function. The propagation in time span $\tau > 0$ of densities in the configuration space can be given by a linear self-adjoint Markov transfer operator [Web11] $\mathcal{P} : L^{1,2}_{\pi_q}(\Omega) \to L^{1,2}_{\pi_q}(\Omega)$. The construction of this transfer

operator is based on a non-linear and possibly stochastic dynamics of the system. We define for a given micro state (q,p) the probability density function $\Phi^{-\tau}(\widetilde{q}|(q,p))$ in $\widetilde{q}$. With this probability the system being in state q and momentum p switches to $\widetilde{q}$ in time τ. The transfer operator is given by

$$\mathcal{P}(\tau)f(q) = \int_{\mathbb{R}^{3N}} \left(\int_{\Omega} f(\widetilde{q}) \Phi^{-\tau}(\widetilde{q}|(q,p)) d\widetilde{q} \right) \pi_p(p) dp. \tag{2.5}$$

We remark, that for deterministic dynamics Φ is the Dirac delta. The self-adjointness of this transfer operator stems from the assumption, that for every "trajectory" from q to $\widetilde{q}$ there exists in the equilibrium ensemble a reverse trajectory with the same probability (detailed balance condition). The relation between the operator $\mathcal{P}(\tau)$ acting on membership functions and the density propagating Markov operator $\bar{\mathcal{P}}$ is given by [Web11]

$$\bar{\mathcal{P}}(\tau) = \pi_q \circ \mathcal{P}(\tau) \circ (\pi_q)^{-1}.$$

It has been shown by Weber [Web11], that the operator $\mathcal{P}(\tau)$ which satisfies the detailed balance equation, is self-adjoint with respect to the π_q weighted scalar product $\langle g, f \rangle_\pi = \int_\Omega f(q)g(q)\pi(q)\, dq$, that is

$$\langle g, \mathcal{P}(\tau)f \rangle_\pi = \langle \mathcal{P}(\tau)g, f \rangle_\pi,$$

and has a real valued spectrum $\sigma(\mathcal{P}) \subset [-1,1]$. Moreover the operator $\mathcal{P}(\tau)$ is assumed to have a discrete spectrum of eigenvalues $1 = \lambda_1 \geq \lambda_2 \geq ... \geq \lambda_n$, in particular we assume that there exists a set of eigenvalues $\{\lambda_1, ..., \lambda_n\}$ close to 1. Their corresponding eigenfunctions are denoted by $\mathcal{X} = \{\mathcal{X}_1, ..., \mathcal{X}_n\}$, such that $\mathcal{P}(\tau)\mathcal{X} = \mathcal{X}\Lambda$, where $\Lambda = \mathrm{diag}(\lambda_1, ..., \lambda_n)$. We now aim to reveal the underlying discrete Markov state model, where each macro state is one possible Markov state and the transition behavior is given by an $n \times n$ row-stochastic transition matrix $P(\tau)$. Thus, we need to determine the size and shape of the macro states, i.e. the membership functions χ, which we have not done yet. Moreover, it has to be guaranteed that the discrete model is Markovian. More clearly, the time-discretized process in the continuous space of micro states is Markovian (operator $\mathcal{P}$). However, the time-series of projected densities of micro states at time $0, \tau, 2\tau, \ldots$ (projected to a finite set of macro states) may be non-Markovian. It is known, that the projection onto a finite dimensional state space has to be taken with care, since in general the underlying discrete process is not necessarily Markovian, see [SNS10]. It has been shown [Web11] that for the choice $\chi = \mathcal{X}A$ (χ is a linear combination of the eigenfunctions $\mathcal{X}$) the Markovianity can be preserved. In particular

$$\chi_j(q) = \sum_{i=1}^{N} A_{ij} \mathcal{X}_i(q), \qquad j = 1, ..., n, \tag{2.6}$$

where $A = \{A_{ij}\}_{i,j=1,...,n}$ is a non-singular transformation matrix and $\{\mathcal{X}_i\}_{i=1,...,n}$ the above mentioned eigenfunctions. This matrix A is the solution of a convex maximization problem called PCCA+ (Perron Cluster Analysis). For details we refer to [Web06, DW05, FRSW11]. We remark, that individual eigenfunctions $\mathcal{X}$ do not overlap since they are orthogonal, but the membership functions χ_i as linear combinations of the eigenfunctions might have an overlap. The Markov property of the projected time-series is preserved, if we use the following Galerkin projection [KW07]:

$$P(\tau) = (\langle \chi, \chi \rangle_\pi)^{-1} (\langle \chi, \mathcal{P}(\tau)\chi \rangle_\pi), \tag{2.7}$$

where $\langle \chi, \chi \rangle_\pi$ and $\langle \chi, \mathcal{P}(\tau)\chi \rangle_\pi$ are $n \times n$-matrices given by considering all pairs χ_i, χ_j, with $i, j \in \{1, \ldots, n\}$. Markovianity can be expressed by the fact that $P(s\tau) = P(\tau)^s, s \in \mathbb{N}$. The above projection reflects the correct dynamical long term behavior of densities in the original micro system. The matrix $P(\tau)$ given by (2.7) represents, therefore, the correct Markov State Model which also captures the spatial effects. Let now $D = \mathrm{diag}(w_1, ..., w_n)$ be the $n \times n$ diagonal matrix of the statistical weights in (2.2), then we can define two row-stochastic matrices

$$T = D^{-1}\langle \chi, \mathcal{P}(\tau)\chi \rangle_\pi = D^{-1}A^T \Lambda A \quad \text{and} \quad S = D^{-1}\langle \chi, \chi \rangle_\pi = D^{-1}A^T A, \tag{2.8}$$

see [Web11]. By using membership functions, a macro state of the system is not a subset in conformational space. A macro state i is like a part of the ensemble given by the density function $\chi_i \cdot \pi_q$, which might be interpreted as a sub-density of the ensemble. The matrix T can be interpreted in the following sense: T_{ij} denotes the relative portion of the sub-density $\chi_i \cdot \pi_q$ that can be found in χ_j after propagating it in the time-span τ. This would correspond to our "usual" definition of a transition matrix. Taking this matrix as a basis of a Markov chain would not lead to the correct long term behavior of the micro states. The error is due to the recrossing events. The relation between the matrix T, which can be interpreted as a transition matrix, and the correct projection $P(\tau)$ is given by: $P(\tau) = S^{-1}T$. The more the matrix S differs from identity the more the correct projection $P(\tau)$ differs from the transition matrix T. Thus, the rebinding effect can be measured by the matrix S. In order to derive this matrix from simulation data, we investigate transition rates instead of transition probabilities. The operator $\mathcal{P}(\tau)$ defines a time-independent operator $\mathcal{Q}$ by

$$\mathcal{Q} = \lim_{\tau \to 0+} \frac{\mathcal{P}(\tau) - \mathcal{I}}{\tau} \tag{2.9}$$

where $\mathcal{I}$ is the identity operator. If we assume that $\mathcal{P}$ meets the Chapman Kolmogorov equation, that is $\mathcal{P}(\tau_1 + \tau_2) = \mathcal{P}(\tau_1)\mathcal{P}(\tau_2)$ for $\tau_1, \tau_2 > 0$ then $\mathcal{Q}$ is the infinitesimal generator of $\mathcal{P}$:

$$\mathcal{P}(\tau) = \exp(\tau \mathcal{Q}).$$

For a crisp, i.e. set-based, discretization there exists no infinitesimal generator in general. However, it has been shown that for a discretization in terms of membership functions there exists an infinitesimal generator [Web11]. Since the eigenfunctions of $\mathcal{Q}$ and $\mathcal{P}$ are the same and the eigenvalues $\{\xi_i\}_i$ of $\mathcal{Q}$ meet $\exp(\xi_i) = \lambda_i$, we can employ the Galerkin discretization in the fashion of (2.7) by an $n \times n$-rate matrix

$$Q_c = A^{-1}\Xi A = (\langle \chi, \chi \rangle_\pi)^{-1}\langle \chi, \mathcal{Q}\chi \rangle_\pi, \tag{2.10}$$

preserving the Chapman-Kolmogorov property [Web11, Web13]. Here the diagonal matrix Ξ contains the leading eigenvalues $0 = \xi_1 > \xi_2 \geq \xi_3 \ldots \geq \xi_n$ of $\mathcal{Q}$ and A is the above defined real $n \times n$-transformation matrix, which transforms the eigenfunctions of the infinitesimal generator $\mathcal{Q}$ into membership functions of the macro states. The computation of eigenfunctions of some continuous operator $\mathcal{Q}$ is in general is a challenging numerical task. There exist adaptive schemes for an approximation of such functions in the context of molecular simulation [Web11]. For the applications shown in this article, we assume to either analyze discrete systems or to be able to estimate Q_c on the basis of experimental data.

3. Deriving the minimal rebinding effect from a given kinetics. In section one we explained on a simple example that the Markov property can be destroyed by the rebinding effect. Moreover we motivated that knowing the rebinding effect is demanded for a suitable and reliable simulation of the binding process. In this section we provide a tool, for detecting the minimal rebinding effect spoiling the Markov property. As it turns out the magnitude of the overlap between the conformations seems to be an adequate indicator.

For sake of simplicity, we assume that the transition rates Q_c can be measured experimentally. We are interested in the (time-independent) entries of Q_c in the case of an equilibrated molecular system. The eigenvalues ξ_i of this matrix represent the dominant time-scales of the molecular system. If these eigenvalues are close to zero then the holding probabilities of the macro states are almost one. The macro states are very stable. The trace of Q_c is independent from A and identical to the sum of the leading eigenvalues of $\mathcal{Q}$. We define the quantity $F := -\text{trace}(Q_c)$ as an indicator for the stability of the molecular system: The higher F the less stable is the molecular system. The higher the quantity the "faster" and less stable is the molecular system. Furthermore,

$$\begin{aligned} F = -\text{trace}(Q_c) &= -\tau^{-1}\log(\exp(\text{trace}(\tau Q_c))) \\ &= -\tau^{-1}\log(\det(\exp(\tau Q_c))) \\ &= -\tau^{-1}\log(\det(P(\tau))) \\ &= \tau^{-1}(\log(\det(S)) - \log(\det(T))), \end{aligned} \tag{3.1}$$

where S and T are given by (2.8). The higher the outer diagonal elements of the transition matrix T, the faster is the process. This is an expected behavior. The "unexpected" part of the quantity F is, that the overlap of different macro states (off-diagonal elements of the S-matrix) have an influence, too. Furthermore, this influence is the opposite of T, a higher overlap in S means slower processes. A low value of $\det(S)$ leads to a low value of F. This is due to the rebinding. A low $\det(S)$ value indicates a high rebinding effect. A system with strong rebinding effects is more stable which has also been observed in the context of protein folding (and recrossing) [Kri11].

3.1. Idea of solving an optimization problem. We remark, that the eigenvalues of the infinitesimal generator $\mathcal{Q}$ are also eigenvalues of Q_c because of (2.10). The (left) eigenvalue problem is

$$Q_c X = X\Xi, \tag{3.2}$$

where $X \in \mathbb{R}^{n\times n}$ contains the corresponding eigenvectors X_i. Note that the first eigenvector is given by $X_1 := (1,\dots,1)^T$. We show in the following that knowing these eigenvectors is sufficient for estimating the minimal rebinding effect of the corresponding kinetics.

Comparing equations (2.10) and (3.2), one can see that the columns of A^{-1} are also eigenvectors of Q_c. According to [Web06], the first row of A is given by the statistical weights of the clusters. Their sum is 1. Thus, the first column of A^{-1} has to be identical to X_1 (because of $AA^{-1} = I$), whereas the other columns of A^{-1} can be arbitrary multiples of the eigenvectors X_i:

$$A^{-1} = \begin{pmatrix} 1 & & & \\ \vdots & \alpha_2 X_2 & \cdots & \alpha_n X_n \\ 1 & & & \end{pmatrix}, \tag{3.3}$$

with $\alpha_2, \ldots, \alpha_n \in \mathbb{R}$.

Our aim was to estimate the minimal rebinding effect included in Q_c. The overlap matrix S of the membership functions should be considered to be as close as possible to the identity matrix. Let us recall, that the entries of the matrix S are non-negative, because of the non-negativity of the membership functions. If we take the equations (3.2), (3.3), and (2.8) into account, the resulting minimization problem is

$$\min_{\alpha_1,\ldots,\alpha_n \in \mathbb{R}} |\det(S) - 1| \tag{3.4a}$$

$$\text{such that} \qquad \alpha_1 = 1, \tag{3.4b}$$

$$A_{ij}^{-1} = \alpha_i X_{ij}, \ \forall_{i,j} \tag{3.4c}$$

$$S = D^{-1} A^T A, \tag{3.4d}$$

$$S_{ij} \geq 0 \ \forall_{i,j}. \tag{3.4e}$$

Here, the constraints (3.4b) and (3.4c) are given by (3.3), the condition (3.4d) determines the structure of S and (3.4e) ensures the positivity of S.

Thus, in order to estimate the minimal rebinding effect that is included in a given kinetics Q_c, one has to compute the eigenvectors X_i of Q_c first, and then to solve the optimization problem (3.4). The result is an optimal overlap matrix S_{opt} with $\det(S_{real}) \leq \det(S_{opt}) \leq 1$, where S_{real} denotes the real overlap matrix (the real rebinding effect). The smaller the determinant of S_{opt}, the smaller is the determinant of S_{real} and the more intensive is the rebinding effect.

Unfortunately, this method only gives non-trivial estimates for $n > 2$. In the case of $n = 2$, the side constraints of Q_c (row sum is zero, the statistical weights of the clusters are stationary) lead to the fact, that Q_c is a reversible matrix, i.e., $DQ_c = Q_c^T D$, where $D \in \mathbb{R}^{n \times n}$ is the diagonal matrix of the statistical weights of the clusters. The following theorem shows that in this case, the estimation is $\det(S_{opt}) = 1$.

THEOREM 1. *Let the matrix $Q_c \in \mathbb{R}^{n \times n}$ be reversible. Furthermore, let Q_c stem from a clustering with positive definite overlap matrix S. Then there exists a feasible matrix $A \in \mathbb{R}^{n \times n}$ in the above optimization problem (3.4) with* $\det(S_{opt}) = \det(D^{-1} A^T A) = 1$.

Proof. Let Q_c be generated by a regular matrix B, i.e. $Q_c = B^{-1} \Xi B$. Since Q_c is reversible we have

$$DQ_c = DB^{-1}\Xi B = B^T \Xi B^{-T} D = Q_c^T D \tag{3.5}$$

Multiplying both sides of (3.5) by D^{-1} and defining $C = B^{-T} D$ we obtain

$$Q_c = D^{-1} B^T \Xi B^{-T} D = C^{-1} \Xi C.$$

Since $Q_c = B^{-1}\Xi B$ there exists a diagonal matrix $M = \operatorname{diag}(m_1, ..., m_m)$ such that $C^{-1} = B^{-1} M$. The entries of M are real and positive since $S = D^{-1} B^T B = C^{-1} B = B^{-1} M B$ and therefore $\widetilde{M} = \operatorname{diag}(\sqrt{m_1}, ..., \sqrt{m_n}))$ is also a real positive diagonal matrix. Define $A := \widetilde{M}^{-1} B$. This matrix is feasible according to the optimization problem (3.4), because the columns of A^{-1} (like the columns of B^{-1}) are multiples of the eigenvectors of Q_c with $\widetilde{M}_{11}^{-1} = 1$.

The following equations hold (and also show the feasibility of S_{opt}):

$$D^{-1} A^T A = D^{-1} B^T \widetilde{M}^{-1} \widetilde{M}^{-1} B$$

$$= D^{-1}B^T M^{-1}B$$
$$= C^{-1}M^{-1}B$$
$$= B^{-1}MM^{-1}B = I,$$

where I is the $n \times n$-identity matrix. □

For a reversible example, the estimation (3.4) is trivial. In the general case, the estimate can be good or bad, see Fig. 3.1. The randomly generated matrices Q_c in

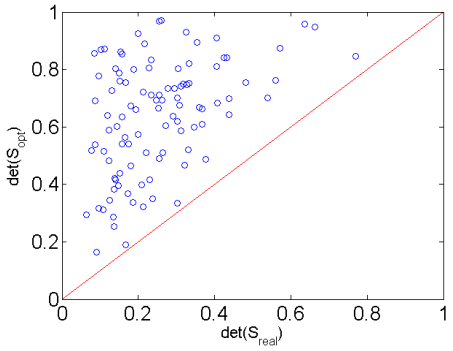

FIG. 3.1. *100 randomly sampled feasible* 3×3*-transformation matrices* A *are used to test the estimation quality of the optimization problem (3.4). It can be seen that* $\det(S_{opt})$ *is in fact an upper bound of* $\det(S_{real})$*, but the approximation quality can be rather bad or sharp (the sampled examples "fill the whole triangle").*

Fig. 3.1 often have negative off-diagonal entries, although the overlap matrix S was constructed to be positive and also positive-definite. Note that S^{-1} can transform a sparse matrix $D^{-1}\langle\chi, \mathcal{Q}\chi\rangle_\pi$ with non-negative off-diagonal elements into a dense matrix with possibly negative off-diagonal entries (negative transition rates). Thus, in order to derive Q_c from experimental data, one has to take dense matrices Q_c and also negative transition rates (for their correct reconstruction) into account. In Fig. 3.2 one can see that the estimate $\det(S_{opt})$ correlates with the "grade of non-reversibility" and the minimal transition rates of the matrix Q_c.

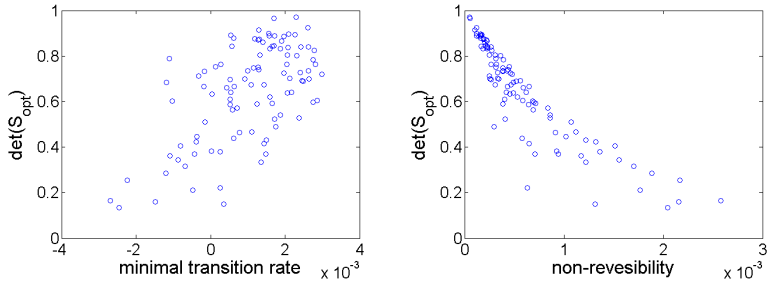

FIG. 3.2. *100 randomly sampled feasible* 3×3*-transformation matrices* A *are used for the construction of* Q_c*.* S_{opt} *is determined by the optimization problem (3.4). Left: The rebinding effect* $\det(S_{opt})$ *is compared to the minimal transition rate in* Q_c *(for the construction of* Q_c*, always the same eigenvalues are used* $\xi_1 = 0, \xi_2 = -0.01, \xi_3 = -0.02$*). Right: The non-reversibility is measured by* $\|DQ_c - Q_c^T D\|$ *and compared to* $\det(S_{opt})$*. There is a strong correlation between these two quantities.*

3.2. Reformulation of the optimization problem. The optimization problem (3.4) can have many local solutions. In order to solve it, a multistart local optimization procedure may be suitable. Some illustrative examples in Section 4 and the entries in Figure 3.2 are solved in that way.

For high-dimensional problems (more than three states), however, a random multistart algorithm may miss the global optimum. In this section, the optimization problem (3.4) is transformed into a linear program (3.12), which can be solved alternatively and has a slightly different objective function.

The columns of A^{-1} are (right) eigenvectors of Q_c, which may be expressed by

$$A^{-1} = XU, \tag{3.6}$$

where X is the eigenvector matrix of Q_c and $U = \mathrm{diag}(\alpha_1, \ldots, \alpha_n)$ is the diagonal matrix of the optimization variables α_i and $\alpha_1 = 1$.

Alternatively, one can see from equation (2.10) that A^T is also a matrix of left eigenvectors of Q_c, which can be expressed by

$$A = \bar{U}Y^T, \tag{3.7}$$

where Y is the matrix of the left eigenvectors of Q_c and $\bar{U} = \mathrm{diag}(\bar{\alpha}_1, \ldots, \bar{\alpha}_n)$ is the diagonal matrix of the alternative optimization variables $\bar{\alpha}_i$. Note, that $\bar{\alpha}_1 = 1$ because the first row of A consists of the statistical weights of the clusters and, therefore, is identical to the leading left eigenvector of Q_c (stationary density).

With these preparations, we first change the objective function of (3.4). Instead of minimizing the expression $|\det(S) - 1|$, one can simply maximize $\det(S)$. The reason is, that the entries of S are non-negative (according to the constraints) and the row sums of S are equal to one (for every row), which will be shown now. Thus, the eigenvalues of S (Gershgorin estimate) lie inside the interval $[-1, 1]$. Therefore, $\det(S) \leq 1$.

THEOREM 2. *In the optimization problem (3.4) the row sums of the non-negative matrix S are 1 by construction. Thus, $\det(S) \leq 1$ and $\mathrm{trace}(S) \leq n$. Identity only holds if S is the unit matrix.*

Proof. For the proof we need two different vectors. The vector e is a constant vector consisting of the entries 1. The first entry of the vector e_1 is 1, all other entries are 0. We will complete the proof in two steps. First, we show $Ae = e_1$:

$$\begin{aligned} XU = A^{-1} &\Rightarrow A = U^{-1}X^{-1} \\ &\Rightarrow Ae = U^{-1}X^{-1}e \\ &\Rightarrow XUAe = e, \end{aligned} \tag{3.8}$$

since X consist of the (linear independent, right) eigenvectors of Q_c and the first eigenvector is e, we get $UAe = e_1$. With $\alpha_1 = 1$ we arrive at $Ae = e_1$. Second, we show that $D^{-1}A^T e_1 = e$ and complete the proof.

$$D^{-1}A^T e_1 = D^{-1}Y\bar{U}e_1 = D^{-1}Ye_1 = e, \tag{3.9}$$

where we have used that $\bar{\alpha}_1 = 1$ and that the diagonal matrix D consists of the elements of the first row of Y (stationary density). □

The optimization problem (3.4) tries to find a matrix S which is a close as possible to the identity matrix. Instead of maximizing $\det(S)$, one can also maximize $\mathrm{trace}(S)$ according to Theorem 2. The objective function is:

$$\mathrm{trace}(S) = \mathrm{trace}(D^{-1}A^T A)$$

$$= \operatorname{trace}(D^{-1}Y\bar{U}^2Y^T)$$
$$= \sum_{i=1}^{n}\sum_{k=1}^{n}\bar{\alpha}_k^2\frac{y_{ik}^2}{y_{k1}}. \tag{3.10}$$

The side constraints for $i \neq j$ are:

$$S_{ij} = \sum_{k=1}^{n}\bar{\alpha}_k^2\, y_{ik}\, y_{jk} \geq 0. \tag{3.11}$$

We get a linear program by substitution $\beta_i = \bar{\alpha}_i^2$ (substitution in the objective function (3.10) and in the constraints (3.11)). We have to add the positivity constraints $\beta_i \geq 0$ and $\beta_1 = 1$. The complete optimization problem is:

$$\max_{\beta}\sum_{k=1}^{n}\beta_k\Big(\sum_{i=1}^{n}\frac{y_{ik}^2}{y_{k1}}\Big)$$

$$s.t. \beta_i \geq 0, \beta_1 = 1,$$

$$\sum_{k=1}^{n}\beta_k\, y_{ik}\, y_{jk} \geq 0. \tag{3.12}$$

An optimal solution β provides an optimal matrix $S_{opt} = D^{-1}YBY^T$, where B is the diagonal matrix of the entries of β.

4. Illustrative Examples. In this section, we give examples, which show the performance of our method.

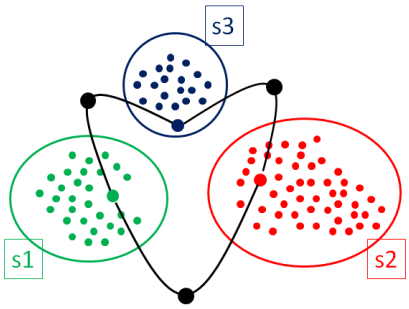

FIG. 4.1. *Artificial example: A transition graph. The corresponding transition network consists of three sets of complete graphs. The complete graphs have a different number of vertices, but all transitions (edges) have the same rate. Each set is connected to the other sets by transition vertices (black). The rates to and from the transition vertices are ten times higher that the rates within the sets (lower statistical weight of the transition vertices).*

4.1. A transition network graph. Only if the kinetics Q_c of a system is non-reversible, a non-trivial rebinding effect can be estimated. The rebinding effect that is included in a monovalent ligand-receptor binding kinetics is non-detectable from the corresponding kinetics data (concentration vs. time), if it has only two distinguishable

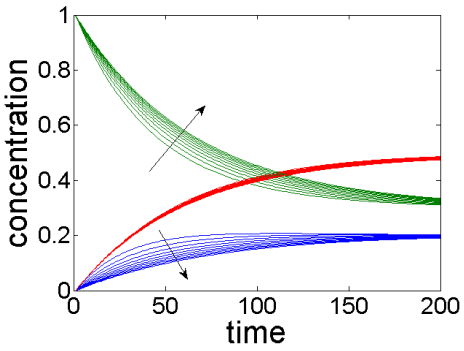

FIG. 4.2. *Concentration curves of the illustrative example with increasing number of transition vertices between set 1 and set 2. The more transition vertices are inserted (see arrows) the more the equilibration between set 1 (green curves) and set 2 (blue curves) is slowed down compared to the equilibration time of set 3 (red curves). By this slowing down, the kinetics becomes more and more non-reversible (the minimal rebinding effect increases). Thus, the red curve is like a "baseline" in this example.*

macro states – bound and unbound. The following artificial example (see Fig. 4.1) consists of three macro states. It illustrates the meaning of transition regions for the rebinding effect.

In this example we see three different macro states (metastable regions). Every micro state of these regions is connected to each other micro state of the same region. For constructing the transition rate matrix $\mathcal{Q}$, all edges in these fully connected subgraphs correspond to a transition rate of 1. The transitions between the regions are indicated by black circles (transition vertices) which connect one state of one region with one state of another region. The corresponding transition rates in $\mathcal{Q}$ are set to 10, to make the transition vertices less stable.

The rebinding effect stems from the overlap of the membership functions (=linear combination of the eigenfunctions of $\mathcal{Q}$). This overlap is high if the transitions between the macro states are slow and not "jump-like". If we extend the transition regions between the macro states, the rebinding effect should increase. In order to illustrate this behavior we inserted more and more transition vertices between set 1 and set 2 in the transition network of Fig. 4.1. The kinetics between the three macro states is changed, see Fig. 4.2.

Applying the optimization scheme of eq. (3.4), we can derive the resulting minimal rebinding effect, which is illustrated in Table 4.1. In fact, by slowing down the transitions between the macro states, the rebinding effect increases.

4.2. An artificial bivalent binding process. Binding kinetics is often used to describe the time-dependent binding process of ligand molecules to their receptor molecules. One can discriminate between a monovalent binding process and a multivalent binding process. For the monovalent case, the mathematical modeling of its kinetics is well-understood. In the easiest examples, the association rate is proportional to $[L] \cdot [R]$, i.e., the product of the ligand and the receptor concentrations. The dissociation rate is proportional to $[LR]$ – the concentration of the ligand-receptor-complex. The basic assumption for these proportionalities is a well-stirred reaction tube, which means that ligands and receptors are uniformly distributed. Sometimes, however, there exist many identical receptors presented in a certain spatial arrange-

number of t-vert.	$\det(S_{real})$	$\det(S_{opt})$ (3.4)
1	0.9913	1.0000
2	0.9897	0.9977
3	0.9882	0.9956
4	0.9867	0.9937
5	0.9852	0.9918
6	0.9837	0.9901
7	0.9823	0.9884
8	0.9810	0.9868
9	0.9796	0.9851
10	0.9783	0.9835

TABLE 4.1

Given the number of transition vertices between set 1 and set 2 (1st column) the overlap matrix S_{real} is computed according to PCCA+. The determinant of S_{real} (2nd column) is estimated from above by the result $\det(S_{opt})$ of the optimization problem (3.4). One can see that the optimization problem gives feasible upper bounds for $\det(S_{real})$. Both values are decreasing with an increasing number of transition vertices. Interestingly, the optimization problem (3.12) gives the same results. The reason is that the optimum is attained at a vertex of the feasible set. This set is identical in (3.4) and (3.12). In the general case, the results may differ.

ment (e.g., by dimerization of a protein or by assembly on a cell surface), such that it is possible to address neighboring receptors with ligands. A direct consequence is, that the receptors are not spatially uniformly distributed. Whenever the receptor molecules are spatially pre-organized, the corresponding binding process is denoted as multivalent. Especially, the bivalent or the polyvalent case are often observed in nature. These systems are of high interest for pharmaceutical and technical applications. If the ligands are linked to each other in an appropriate way to match the pre-organized receptor molecules and, thus, are also presented multivalently, then extremely high binding affinities are often observed.

A "straight forward" kinetic model for the multivalent binding process is given by counting the binding events. As an example, for a bivalent ligand binding to a bivalent receptor this means that there exist three macro states: The unbound state, the singly bound state and the doubly bound state. This model is represented by the following two reversible reactions:

$$\begin{aligned} LL + RR &\leftrightharpoons L(LR)R, \\ L(LR)R &\leftrightharpoons (LRLR), \end{aligned} \tag{4.1}$$

where $L(LR)R$ denotes the singly bound macro state and $(LRLR)$ is the doubly bound macro state.

Section 4.1 has illustrated that slowing down the time scale of the transitions between the macro states compared to the self-equilibration time within the macro states leads to a increasing rebinding effect ($\det(S_{real})$ and $\det(S_{opt})$ decrease). We will illustrate what this means for a bivalent binding process. The reactions (4.1) are the standard approach to model a bivalent binding process. We will add another reaction to this model:

$$LL + RR \leftrightharpoons (LRLR), \tag{4.2}$$

where we assume a direct transition from a unbound situation to a doubly bound macro state. We have to add this further direct reaction to end up with a dense matrix

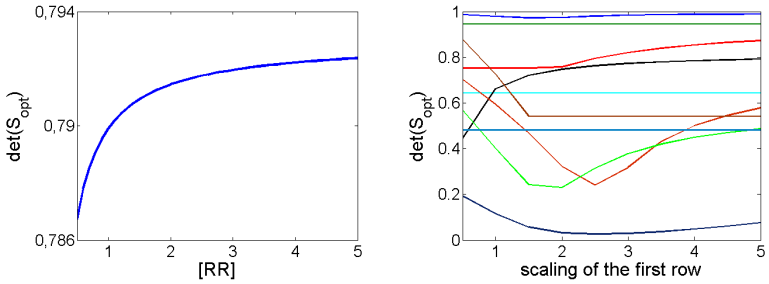

FIG. 4.3. *Left: The minimal rebinding effect of Q_c depends on the concentration [RR] of the receptor molecules. The determinant $\det(S_{opt})$ increases with [RR]. Thus, the minimal rebinding effect decreases with higher concentrations of the receptor molecules. Right: For arbitrary sampled feasible Q_c-matrices, the minimal rebinding effect can depend on the scaling of the first row of Q_c in different ways.*

Q_c, which has to be assumed according to the theory. S^{-1} turns a sparse Galerkin projection of an infinitesimal generator $\mathcal{Q}$ into a dense matrix Q_c. Let's say that we have (by parameter optimization) fitted reaction rates of all these equations to a given experimental time-concentration-plot, where we have measured the concentrations in $\frac{\text{mol}}{l}$ and the time in nanoseconds.

- For the reaction "0 =unbound $\leftrightarrow$ 1 =singly bound" we get $k_{01} = 0.99\frac{l}{\text{mol}\cdot\text{ns}}$ and $k_{10} = 0.1\frac{1}{\text{ns}}$.
- For the reaction "1 =singly bound $\leftrightarrow$ 2 =doubly bound" we get $k_{12} = 0.3\frac{1}{\text{ns}}$ and $k_{21} = 0.01\frac{1}{\text{ns}}$.
- For the reaction "0 =unbound $\leftrightarrow$ 2 =doubly bound" we get $k_{02} = 0.01\frac{l}{\text{mol}\cdot\text{ns}}$ and $k_{20} = 0.001\frac{1}{\text{ns}}$.

If we insert these quantities into the rate matrix Q_c, we arrive at:

$$Q_c = \begin{pmatrix} -(k_{01}+k_{02})[\text{RR}] & k_{01}[\text{RR}] & k_{02}[\text{RR}] \\ k_{10} & -(k_{10}+k_{12}) & k_{12} \\ k_{20} & k_{21} & -(k_{20}+k_{21}) \end{pmatrix}$$
$$= \begin{pmatrix} -1[\text{RR}] & 0.99[\text{RR}] & 0.01[\text{RR}] \\ 0.1 & -0.4 & 0.3 \\ 0.001 & 0.01 & -0.011 \end{pmatrix},$$

which has the unit ns^{-1}. The matrix Q_c depends on the concentration of the bivalent receptor molecules [RR]. The kinetics equation is $\dot{x}^T = x^T Q_c$, where x is the concentration vector consisting of the concentrations [LL],[L(LR)R] and [(LRLR)]. It is reasonable that the rebinding effect depends on the concentration of the receptor molecules according to the results of the last section. The concentration of the receptors determine the "size" of the transition regions between the binding events (from the perspective of the ligand). In Fig.4.3 (left) one can see for the constructed example that the rebinding effect decreases if the receptor concentration increases. This behavior can not be observed for arbitrary 3×3-matrices Q_c, see Fig.4.3 (right), but in our example an increase of the receptor concentration leads to a decrease of the transition regions between the binding events and, thus, to a decreasing rebinding effect according to section 4.1.

It is counter-intuitive to say that "less receptors means more rebinding" and, therefore, this insight needs a short explanation. In the constructed example of this

section, we basically assumed that the kinetic model (given by eq. (4.1) and eq. (4.2)) is correct. This means, the unbinding of a ligand from one receptor and its binding to another receptor are two kinetically distinguishable events. If one expects that the rebinding effect increases if more receptors are available, then (from a mathematical point of view) it is meant that the binding events between different receptors are considered to be kinetically more or less indistinguishable. Instead of analyzing the dependence of the rebinding effect on the receptor concentration, one has to analyze the dependence of the correct kinetic model (leading eigenfunctions of the infinitesimal generator) on the experimental setting of the molecular system. In order to understand this, look at Figure 4.4. A bivalent ligand (doubly) bound to a bivalent receptor is shown. It is the example of an HIV protease inhibitor binding to the HIV-1-protease receptor [KBBD93].

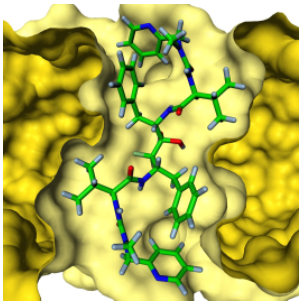

FIG. 4.4. *A symmetry-based HIV protease inhibitor (A-77003) binding to the HIV-1-protease receptor. The inhibitor consist of two equivalent binding sites connected by a single CC-bond. This ligand can not be "singly bound".*

In this case the singly bound macro state does not exist: If one ligand is bound to its receptor, the second ligand is perfectly "pre-organized" such that it is in its bound state too. One can imagine that in many other cases the singly bound state may be seen as a transient state of a bivalent system and not as an own kinetic entity. Thus, the kinetic model which counts the binding events may be too complex for given ligand-receptor-systems. However, the model can also be too simple. In literature there also exist more complicated models of this bivalent binding process, which not only discriminate between a bound and an unbound ligand but also introduce a state (or more states) denoted as "almost bound". The more complicated models are constructed in order to correctly include rebinding effects.

For all these reasons, straight forward binding kinetics may be an insufficient model for a bi- or trivalent binding process. For a polyvalent binding process, this model may be completely useless. Imagine a polyvalent ligand which binds to a surface where polyvalent receptors are available. In this case, there are many possibilities for rebinding events, such that the actual number of bounds may be of no interest, whereas, other coordinates (like the distance between the polyvalent ligand to the surface) may be the most relevant parameter for the kinetic model.

4.3. Interconversion rates. Estimating the rebinding effect in a multivalent binding process is in general not possible by the optimization problem (3.4). The reason is given in the last section: the measured concentrations of certain molecular macro states need not coincide with the time-dominating processes of the system, i.e. with the membership functions derived from the leading eigenfunctions of $\mathcal{Q}$. In this section, we will give an example of a recrossing effect. The flame retardant molecule

hexabromocyclododecane (HBCD) is an example in which the measured concentration curves should reflect the dominant processes of the system [KBJN08]. HBCD exists in different stereo isomeric forms. Given a probe of pure (+)-γ-HBCD, this molecule can transform into six different stereo isomeric forms. The time-dominating step is an interconversion step which takes place on a very high energy level. Thus, the concentration-vs.-time-experiment is carried out over a time-span of several hours. The circles in Fig. 4.5 correspond to the experimental results (only the dominant three stereoisomers are shown in different colors). Additionally, the equilibration concentration of the six stereoisomeric forms is known and also used for the parameter fitting in the followings. In the HBCD example, there is a well-known transition

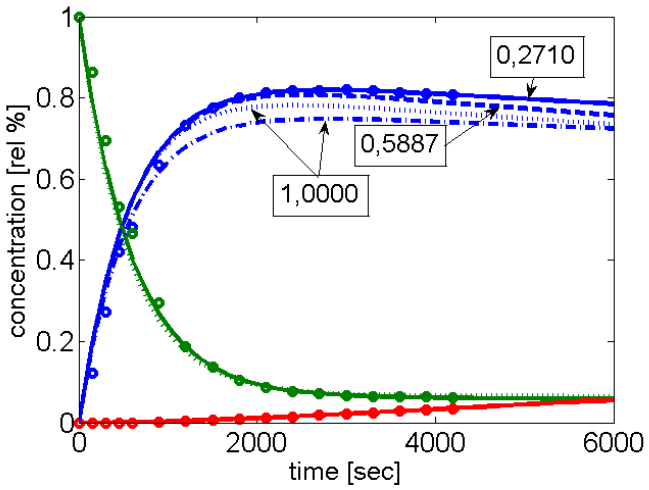

FIG. 4.5. *HBCD interconversion: Optimization results and comparison with experimental data [KBJN08]. The most relevant enantiomers are plotted in different colors ((+)-α-HBCD blue, (-)-α-HBCD red, (+)-γ-HBCD green) and the experimental measurements are included as circles. The solid line represents the best Q_c-fit to the experimental data. The dashed and the dotted lines represent a Q_c-fit which also aims at increasing the reversibility of Q_c (dashed line: small weight of the "reversibility" against fitting the data; dotted line: aiming at a reversible dense matrix Q_c). From a theoretical point of view one would expect a sparse reversible matrix Q_c, if the kinetics does not include a recrossing effect. The best Q_c-fit in this case is given by the dash-dotted line. The numbers in the boxes represent* $\det(S_{opt})$ *for the optimal solution of (3.12). The experimental data can not be fitted with a reversible matrix Q_c, a recrossing effect is probably included.*

micro state. That is a point in conformational space which has to be passed by a HBCD stereoisomer in order to interconvert. The transition regions between the stereoisomers seem to be small in conformational space at a first glance. One would expect jump-like transitions between the stereoisomers (compare Section 4.1) and, thus, a small recrossing effect. At a second glace the things are more complicated. In order to interconvert from one stereoisomeric form into another, HBCD has to exist in a special conformation (trans-position of certain atoms). Furthermore, there exist lower energy barriers between these conformations. For example, after HBCD has interconverted from (+)-γ-HBCD into (+)-α-HBCD, it has to change its conformation before it can further transform into (−)-β-HBCD. These smaller energy barriers lead to extended transition regions between the HBCD stereoisomers. Thus, we expect recrossing effects. In Fig. 4.5 interconversion rates are fitted to the experimental data (assuming a dense 6×6-matrix Q_c with probably negative rates). The results almost

coincide with interconversion rates from literature. In literature we can only compare our results to a sparse, non-negative matrix Q_c (some rates are zero). Our fit also explains the experimental data very well (solid line in Fig. 4.5). The optimization problem (3.12) applied to our fitted Q_c leads to a matrix S_{opt} with $\det(S_{opt}) = 0.2710$ – a clear recrossing effect. Could the experimental data also be explained with less recrossing? In order to analyze this, we have included a weighted objective function to our parameter estimation problem. The fitted matrix Q_c should also be "more" reversible in order to decrease the recrossing effect (see Theorem 1). The dashed line in Fig. 4.5 is the result if we include this further objective to the parameter estimation problem. In this case, $\det(S_{opt}) = 0.5887$ – still a recrossing effect. If we insist on a reversible, dense matrix Q_c and, thus, try to explain the data without any recrossing effect, one would end up with the dotted line in Fig. 4.5. This line does not coincide with the experimental data. Even worse: We also tried to explain the data with a reversible, sparse matrix Q_c. The reason is, that if S is the identity, then Q_c has to be sparse for this special chemical example (only special reactions are possible). The corresponding best fit (dash-dotted line) is clearly different from the experimental result. Thus, the HBCD-experiment can not be understood without recrossing.

5. Conclusion. Kinetics is usually said to be a "non-spatial" model of the processes of a molecular system. However, experimentally measured kinetics includes spatial information indirectly. A ligand which is close to its receptor contributes to the association constant k_a more than a ligand which is far away. The correct weighting in this sense is done by membership functions. A microstate of a molecular system more or less belongs to different macro states. The overlap S of these membership functions scales up the observed stability of the system (via $\det(S)$). The more the membership functions overlap, the more stable the macro states appear to be. In this paper, we have derived a method which is able to estimate the minimal overlap between the membership functions for a given kinetics. This overlap is called "rebinding effect". A ligand which unbinds from its receptor (on the micro level) may still have a high degree of membership to the "bound"-macro state, if the membership functions of the "unbound" and the "bound" state overlap each other. Thus, rebinding is amplified, if and only if the membership functions have a significant overlap. The presented mathematical model allows for a complete and general description of rebinding effects in an equilibrium situation. Taking the mathematical model of membership functions as a basis for analyzing experimental time-concentration curves, one has to fit an assumed dense rate matrix Q_c with possibly negative reaction rates to the given experimental data. Note, that our mathematical model not only includes rebinding effects of ligand-receptor-systems but also general examples of molecular kinetics (see HBCD).

Acknowledgment. Konstantin Fackeldey is supported by the DFG Research Center MATHEON. The work of Marcus Weber has been done for the DFG Collaborative Research Center 765.

REFERENCES

[CS11] Bertrand Care and Hedi Soula. Impact of receptor clustering on ligand binding. BMC Systems Biology, 5(1):48, 2011.

[DDJS99] P. Deuflhard, M. Dellnitz, O. Junge, and Ch. Schütte. Computation of essential molecular dynamics by subdivision techniques. In P. Deuflhard, J. Hermans, B. Leimkuhler, A. E. Mark, S. Reich, and R. D. Skeel, editors, Computational

Molecular Dynamics: Challenges, Methods, Ideas, volume 4 of Lecture Notes in Computational Science and Engineering, pages 98–115. Springer, 1999.

[DHFS00] P. Deuflhard, W. Huisinga, A. Fischer, and Ch. Schuette. Identification of almost invariant aggregates in reversible nearly uncoupled markov chains. Linear Algebra and its Applications, 315(1-3):39 – 59, 2000.

[DW05] P. Deuflhard and M. Weber. Robust perron cluster analysis in conformation dynamics. Linear Algebra and its Applications, 398(0):161 – 184, 2005. Special Issue on Matrices and Mathematical Biology.

[EVE10] W. E and E. Vanden-Eijnden. Transition-path theory and path-finding algorithms for the study of rare events. Ann. Rev. of Phys. Chem., 361:391 – 420, 2010.

[FRSW11] K. Fackeldey, S. Röblitz, O. Scharkoi, and M. Weber. Soft versus hard metastable conformations in molecular simulations. In Particle Methods II Fundamentals and Applications, Proceedings of the International Conference on Particle Based Methods (PARTICLES 2011), pages 899–909, 2011.

[GAS+13] M. Gabba, S. Abbruzzetti, F. Spyrakis, F. Forti, S. Bruno, A. Mozzarelli, F.J. Luque, C. Viappiani, P. Cozzini, M. Nardini, F. Germani, M. Bolognesi, L. Moens, and S. Dewilde. Co rebinding kinetics and molecular dynamics simulations highlight dynamic regulation of internal cavities in human cytoglobin. PLoS ONE, 8, 01 2013.

[GR13] D. Prada Gracia and F. Rao. Rethinking hydrogen-bond kinetics, 2013. arXiv:1308.1030.

[KBBD93] J.J Kort, J.A. Bilello, G. Bauer, and G.L. Drusano. Preclinical evaluation of antiviral activity and toxicity of Abbott A77003, an inhibitor of the human immunodeficiency virus type 1 protease. Antimicrob Agents Chemother, 37(1):115–119, 1993.

[KBJN08] R. Köppen, R. Becker, C. Jung, and I. Nehls. On the thermally induced isomerisation of hexabromocyclododecane stereoisomers. Chemosphere, 71(4):656 – 662, 2008.

[Kri11] Sergei V. Krivov. The free energy landscape analysis of protein (fip35) folding dynamics. The Journal of Physical Chemistry B, 115(42):12315–12324, 2011.

[KW07] S. Kube and M. Weber. A coarse graining method for the identification of transition rates between molecular conformations. J. Chem. Phys., 126(2):0241203, 2007.

[MKMT05] Gopalakrishnan M, Forsten-Williams K, Nugent MA, and UC Täuber. Effects of receptor clustering on ligand dissociation kinetics: theory and simulations. Biophys J., 89(6):3686–3700, 2005.

[RLWW00] J. Rao, J. Lahiri, R. M. Weis, and G. M. Whitesides. Design, synthesis,and characterization of a high-affinity trivalent system derived from vancomycin and l-lys-d-ala-d-ala. J. Am. Chem. Soc., 122:2698– 2710, 2000.

[Sch99] Ch. Schütte. Conformational Dynamics: Modelling, Theory, Algorithm and Application to Biomolecules. Habilitation thesis, Freie Universität Berlin, 1999.

[SNS10] M. Sarich, F. Noe, and Ch. Schütte. On the approximation quality of markov state models. Multiscale Model. Simul., 8(4):1154–1177, 2010.

[Vau10] G. Vauquelin. Rebinding: or why drugs may act longer in vivo than expected from their in vitro target residence time. Expert Opinion on Drug Discovery, 5(10):927–941, 2010.

[VET05] Eric Vanden-Eijnden and Fabio A. Tal. Transition state theory: Variational formulation, dynamical corrections, and error estimates. J. Chem. Phys., 123(18):184103, 2005.

[VL12] G. Vauquelin and I. Van Liefde. Radioligand dissociation measurements: potential interference of rebinding and allosteric mechanisms and physiological relevance of the biological model systems. Expert Opinion on Drug Discovery, 7(7):583–595, 2012.

[WBH12] M. Weber, A. Bujotzek, and R. Haag. Quantifying the rebinding effect in multivalent chemical ligand-receptor systems. Journal of Chemical Physics, 137(5):054111, 2012.

[Web06] M. Weber. Meshless Methods in Conformation Dynamics. PhD thesis, Freie Universität Berlin, 2006.

[Web11] M. Weber. A subspace approach to molecular markov state models via a new infinitesimal generator, 2011. habilitation thesis.

[Web13] M. Weber. Adaptive spectral clustering in molecular simulation. In A. Giusti, G. Ritter, and M. Vichi, editors, Studies in Classification, Data Analysis, and Knowledge Organization, XIV: Classification and Data Mining, pages 147–154, 2013.

[Whi08] A. Whitty. Cooperativity and bioplogical complexity. Nature Chem Bio, 4(8):435–439, 2008. Commentary.